

# Multiwavelength spectroscopy for the detection, identification and quantification of cells

Presented at the SPIE National Meeting East Boston, Massachusetts, 5-8 November 2000.

Yvette D. Mattley<sup>a</sup> and Luis H. Garcia-Rubio<sup>\*a</sup>

<sup>a</sup>Department of Chemical Engineering, University of South Florida, 4202 E. Fowler Avenue, Tampa, FL 33620

## ABSTRACT

Multiwavelength spectroscopy is a rapid technique that provides quantitative information for the detection and identification of cells. A typical multiwavelength spectrum reflects the chemical composition, size, internal structure and number of cells present in a sample. These properties constitute essential information for the identification and classification of cells. The multiwavelength spectrum is generated from the combined scattering and absorption characteristics of the sample. Light scattering theory is then used to deconvolute the spectrum for estimates of the critical parameters necessary for the detection and identification of cells. This approach has been used to determine the spectral fingerprint for blood cells, bacterial cells and protozoa. The characteristic set of optical properties for platelets, *E. coli* and *Cryptosporidium* have been determined as a function of wavelength and used for the quantitative interpretation of UV-vis spectra within the context of Mie theory. The models developed using this approach provide reliable and accurate estimates for cell size, number, chemical composition and internal structure. Information on the chemical composition is further deconvoluted into quantitative estimates of nucleic acid and protein content. This type of detailed information is then used for the discrimination of cell types. The technique is applicable to a wide range of cell types found in diverse environments. Advances in the development of miniaturized spectrometers increase the potential of this method as an excellent candidate for a rapid, reliable and efficient biosensor.

**Keywords:** biosensor, multiwavelength spectroscopy, absorbance, scattering, deconvolution, optical properties, Mie theory, *E. coli*, *Cryptosporidium*, blood cells

## 1. INTRODUCTION

Multiwavelength spectroscopy is a versatile, rapid and reliable tool that has immediate applications as a biosensor for the detection, identification and enumeration of pathogens. The sample information contained in a typical multiwavelength ultraviolet/visible (UV/vis) spectrum includes cell size, chemical composition and shape. This information is obtained from the spectroscopic analysis of a sample measured over a broad range of wavelengths (200 - 900 nm) with scattered light measured at one or many different angles. The ability to extract large amounts of information from a single multiwavelength measurement makes UV/vis spectroscopy a powerful characterization tool. In addition, a spectroscopy-based biosensor provides the added benefits of being rapid, inexpensive and relatively simple to operate.

The spectroscopy approach described in this paper has been used to obtain the correct size distribution for a wide variety of particle based systems including protein aggregates<sup>1</sup>, microorganisms<sup>2,3</sup> and whole blood (Garcia-Rubio unpublished data) and isolated blood components<sup>4</sup>. Identifying particle parameters are obtained for these systems and many others directly from the multiwavelength measurements providing the necessary information for the detection, identification and enumeration of the particles present in the sample. Furthermore, when the multiwavelength measurements are extended to include multiple angles of detection, the shape of the particle can also be obtained providing additional discriminating information.

The approach taken by our group is shown in Figure 1. This approach is based on the fact that particles are characterized by a joint property distribution (JPD). Examples of several important particle properties are included in the figure. In order to

---

\* Correspondence: Email: [garcia@eng.usf.edu](mailto:garcia@eng.usf.edu); Telephone: (813)974-5854 ; Fax:(813)974-3651

identify a particle, information on a range of particle properties must be obtained. We have obtained information on several of these particles properties from simple multiwavelength measurements using a light scattering and absorption interpretation

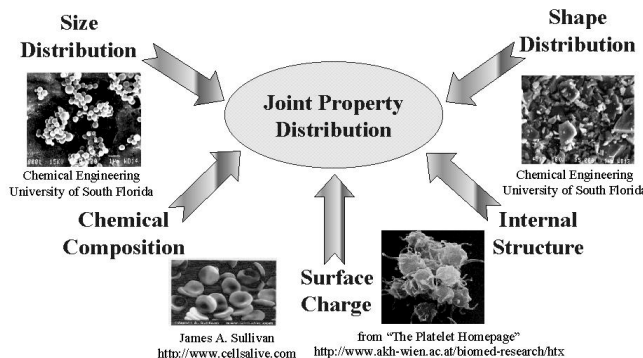


Figure 1: Particles are characterized by a joint property distribution (JPD)

model based on Mie theory. Specifically, this paper reports on the extraction of information relating to the particle size, internal structure and chemical composition for platelets, *E. coli* and *Cryptosporidium* from multiwavelength UV/vis spectroscopic measurements. Note that in addition to these properties, the multiwavelength spectra for these cells contain information that will be useful for further discrimination of particles once the interpretation models are improved and updated.

## 2. THEORY

The transmission spectrum of a particle dispersion contains information that, in principle, can be used to estimate the particle size distribution (PSD) and the chemical composition of the suspended particles. A large number of techniques for the estimation of the PSD from turbidity spectra have been reported<sup>5,6,7,8,9</sup>. Unfortunately, most of these techniques require that either the form of the PSD be known a priori, or that the shape of the PSD be assumed<sup>6,9</sup>. More recently, regularization techniques<sup>10,11,16</sup> applied to the solution of the turbidity equation<sup>12,13</sup> have been demonstrated to yield the correct particle size distribution of a large variety of polymer lattices<sup>14</sup> and protein aggregates<sup>1</sup>, SiO<sub>2</sub> particles<sup>15</sup>, microorganisms<sup>2</sup> and whole blood (Garcia-Rubio unpublished data) and isolated blood components<sup>4</sup>.

The Equation that relates the turbidity ( $\tau(\lambda_0)$ ) measured at a given wavelength  $\lambda_0$  and the normalized particle size distribution for spherical particles ( $f(\mathbf{D})$ ) is given by<sup>5,7</sup>:

$$\tau(\lambda_0) = N_p \left( \frac{\pi}{4} \right) \int_0^\infty Q(\lambda_0, D) D^2 f(D) dD \quad 1$$

Where  $\mathbf{D}$  is the effective particle diameter,  $\mathbf{Q}(\lambda_0, \mathbf{D})$  corresponds to Mie scattering coefficient, and  $N_p$  is the number of particles per unit volume. Equation 1 can be written in matrix form by discretizing the integral with an appropriate quadrature approximation<sup>12,13</sup>:

$$\underline{\tau} = \mathbf{A} \underline{f} + \underline{\epsilon} \quad 2$$

$\underline{\epsilon}$  represents both experimental errors and errors due to the model and the discretization<sup>13</sup>. The regularized solution to Equation 2 is given by:

$$\hat{\underline{f}}(\gamma) = (\mathbf{A}^T \mathbf{A} + \gamma \mathbf{H})^{-1} \mathbf{A}^T \underline{\tau} \quad 3$$

where  $\mathbf{H}$  is a covariance matrix that essentially filters the experimental and the approximation errors ( $\underline{\epsilon}$ );  $\gamma$  is the regularization parameter estimated using the Generalized Cross-Validation technique (GCV)<sup>16</sup>. The Generalized Cross-Validation technique requires the minimization of the following objective function with respect to  $\gamma$ :

$$V(\gamma) = m \frac{\| (I - A(A^T A + \gamma H)^{-1}) \mathbf{t} \|^2}{\text{Trace} [ (I - A(A^T A + \gamma H)^{-1}) A^T J^2 ]} \quad 4$$

Simultaneous application of Equations 3 and 4 to the measured turbidity spectra yields the discretized particle size distribution. The scattering corrected spectra can then be used for composition analysis and/or to fingerprint the absorption characteristics of the particles.

The Mie extinction coefficient ( $\mathbf{Q}_{\text{ext}}(\mathbf{m}(\lambda_0), \mathbf{D})$ ) is a function of the optical properties of the particles and suspending medium through the complex refractive index ( $\mathbf{m}(\lambda_0)$ ) given in Equation 5

$$m(\lambda_0) = \frac{n(\lambda_0) + i\kappa(\lambda_0)}{n_0(\lambda_0)} \quad 5$$

The optical properties of cells were estimated from Equations 1-5. Since the optical properties are implicit functions, an iterative procedure was implemented to estimate them<sup>17</sup>. The optical properties thus obtained were conditional estimates based upon Mie theory, the measured transmission spectrum and the particle counts obtained from a hemocytometer. The refractive index of water ( $\mathbf{n}_0(\lambda_0)$ ) in Equation 5 as a function of wavelength was calculated from the correlation reported by Thormählen et al.<sup>18</sup>. The optical property estimation procedure was as follows: 1) initial estimates of the refractive index were obtained from the reported chemical composition<sup>19,20,21,22</sup> using Equation 5 and the particle counts from the hemocytometer, 2) a transmission spectrum was calculated in the spectral region where no chromophore absorption was expected (400 - 900 nm) and was compared with the measured transmission spectrum at each wavelength, 3) new estimates of the refractive index were obtained using a standard Marquardt-Levenberg algorithm. This iterative procedure continued until the measured and the calculated spectra agreed within the specified tolerance ( $1 \times 10^{-6}$  au).

### 3. METHODS

#### 3.1 Spectroscopy measurements

The UV-vis spectra for cell suspensions were recorded on a diode array spectrophotometer (HP8453, Hewlett Packard, Palo Alto, CA) (having an acceptance angle smaller than  $2^\circ$ ). The instrument records spectra every 0.1 second and averages these spectra over the designated time of sampling (1 to 15 seconds - 10 to 150 spectra averaged). All measurements were conducted at room temperature using a 1 cm path length, 3.5 mL volume quartz cuvette (Starna Cells Inc., Atascadero, CA). Before running each sample, the incident intensity was recorded. Next, in order to account for optical density due only to the sample diluent and the cuvette, the background spectrum for the diluent (deionized water or physiological saline) was measured.

#### 3.2 Generation of extinction spectra

In order to account for small concentration differences between the samples and to simplify the comparison of spectra for different cell samples, extinction spectra were generated by diluting the sample a minimum of 5 times directly in the cuvette. With each diluent addition, the sample was diluted by approximately 15 to 20%. After mixing well by inverting gently, the spectrum was recorded at each concentration. In this manner, five dilutions of the sample were measured with optical densities ranging from 1.2 to 0.1 Au. Beer Lambert Law was then used to calculate the extinction coefficient as a function of wavelength for each sample concentration. The extinction spectra generated in this manner were not only normalized by concentration, but also allowed for the determination of the statistics associated with the calculated extinction coefficients. These statistics could then be used to assess the error associated with the experiment.

### 4. RESULTS

#### 4.1 Multiwavelength UV/vis Spectra for Cells

Qualitative comparison of the multiwavelength transmission spectra for the major blood components and three pathogens reveals the sensitivity and discriminating power of the spectroscopic approach. The transmission spectra in the form of either optical density or extinction spectra are shown in Figure 2 for the major blood components. As shown in this figure for the

major human blood components, the multiwavelength spectra reflect differences in the size shape and chemical composition of the cells. Notice first for plasma, the background fluid component of whole blood, that when the relatively large cells found in whole blood are not present there is no significant scattering observed in the visible region of the spectrum. Note that scattering occurs throughout the entire spectrum but is most easily observed in the visible region (400 to 1100 nm) where little to no absorption occurs. For the other spectra shown in Figure 2, the scattering component is much more significant and determined by the size and shape of the cells.

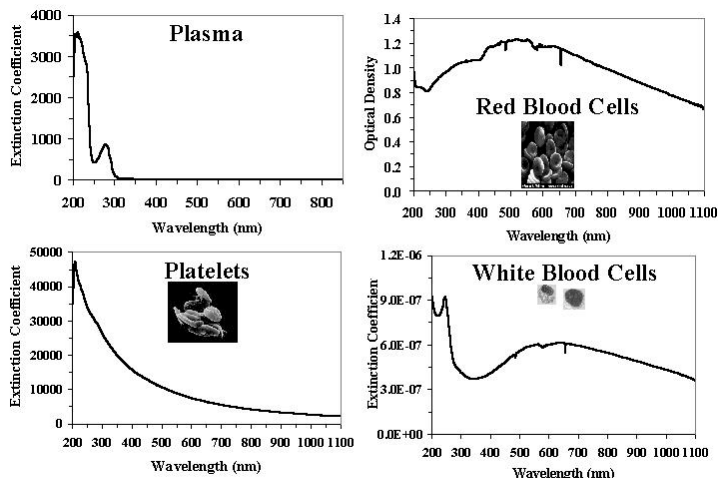


Figure 2: Transmission spectra for isolated human blood components: plasma, red blood cells, platelets and white blood cells

White blood cells are the largest cells found in blood (10 to 22  $\mu\text{m}$ ) and the only cells that contain a highly chromophoric nucleus. White blood cells are spherical in shape. The next largest cells are the 8  $\mu\text{m}$  red blood cells. These biconcave disks are filled with the strong chromophore hemoglobin. Platelets are the smallest cells found in blood. They are 2  $\mu\text{m}$  discoid shaped cell fragments. When the spectra for each of these major blood components are compared, note that these differences in chemical composition, size and shape all translate to significant differences in the multiwavelength spectra shown in Figure 2.

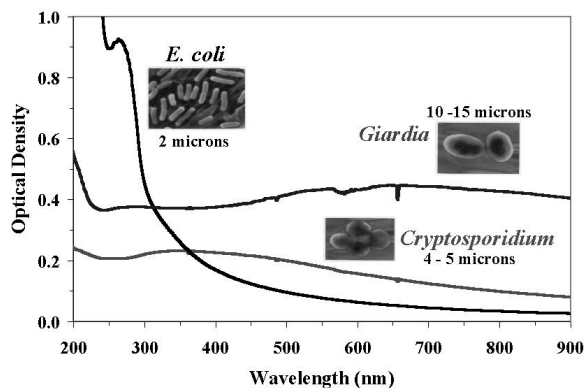


Figure 3: Transmission spectra for three pathogens: *E. coli*, *Giardia* and *Cryptosporidium*

Similar significant spectroscopic differences are observed when multiwavelength transmission spectra for *E. coli*, *Cryptosporidium* and *Giardia* are compared. Notice that the spectra for the pathogens shown in Figure 3 differ from one another and from the spectra for the major blood components shown in Figure 2. As described for Figure 2, the unique spectral fingerprints for these microorganisms arise from differences in the size, shape and chemical composition of the different cells. Clearly even at the qualitative level, multiwavelength UV/vis spectroscopy is able to distinguish different cell types. In the next section, a light scattering and absorption interpretation model based on Mie theory is used to obtain quantitative information for some of these spectra.

#### 4.2 Deconvolution of the Spectra for Platelets, *E. coli* and *Cryptosporidium*

The measured transmission spectra were analyzed using an interpretation model based on Mie theory and the estimated optical properties for cells. The measured optical density spectra represent the combined absorption and scattering properties

of the sample. The interpretation model uses Mie theory to estimate the scattering component of the measured spectrum, which is related to the size, and shape of the particles present in the sample. The absorbance component for the measured spectrum is obtained by subtracting the scattering component estimated with the model from the measured spectrum yielding the scattering corrected spectrum. Estimates for the average size and PSD come from the scattering component and the quantitative information on chemical composition comes from the absorbance component.

In Figure 4, an example of the deconvolution of the transmission spectrum for platelets is shown. Notice that the spectrum calculated with the interpretation model and optical properties is an excellent match for the measured spectrum. The measured and calculated spectra are so similar that the two lines overlay almost perfectly. The model even accounts for the fine details of the spectrum that occur between 400 and 500 nm. The agreement between the measured and calculated spectrum extends throughout the entire wavelength range as shown inset in the plot with the expanded y axis. The level of agreement between the measured and calculated spectrum is indicative of the reliability of the estimates obtained for the model.

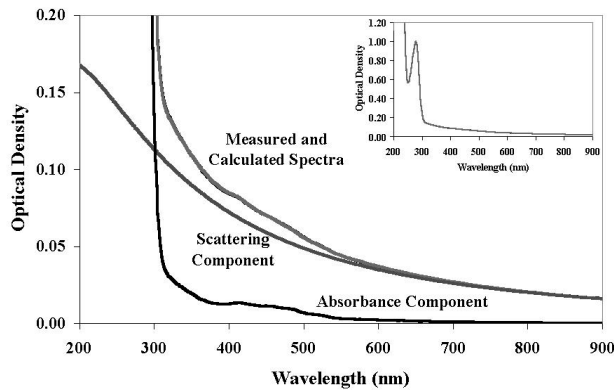


Figure 4: Deconvolution of the platelet rich plasma transmission spectrum

As part of the analysis, the model outputs estimates of the average particle size (2.04  $\mu\text{m}$ ) and number (3.6 million per mL). We have shown that the estimates obtained with the interpretation model agree with impedance based estimates of size and number obtained with a hematology analyzer<sup>4</sup> (Serono Baker 9010+, Allentown, PA). Note that the interpretation model and optical properties have been used with more than 15 different platelet rich plasma samples with similar results and level of agreement between the measured and calculated spectrum.

In addition to platelet rich plasma samples, the interpretation model has also been used for the analysis of transmission spectra for *E. coli* and *Cryptosporidium*. In Figure 5, the results of the analysis of an *E. coli* transmission spectrum with the interpretation model and optical properties is shown. Note that again the interpretation model provides an excellent match for the measured spectrum. As with the analysis of the platelet rich plasma spectrum, the estimate of average size obtained with the interpretation model agrees with literature values reported for *E. coli* (Lenore Hockley Masters thesis in progress).

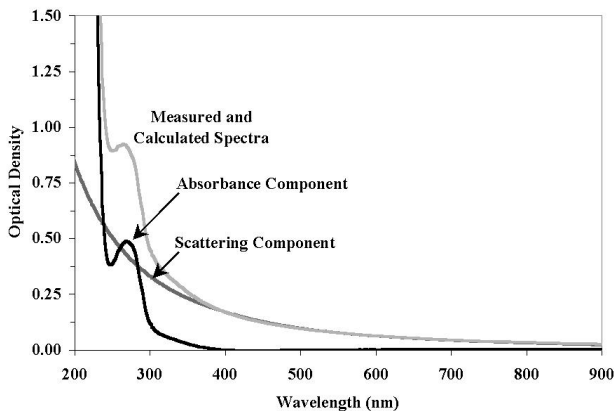


Figure 5: Deconvolution of the transmission spectrum for *E. coli*

Finally, as an example of the most detailed level of analysis possible with our tool, the deconvolution of the transmission spectrum for *Cryptosporidium* is shown in Figure 6. In this case, the absorbance component has been deconvoluted to provide more detailed chemical composition information. In addition to the estimated absorbance and scattering components, the spectrum has been deconvoluted to provide estimates of the protein and nucleic acid content<sup>2</sup>. A sample of

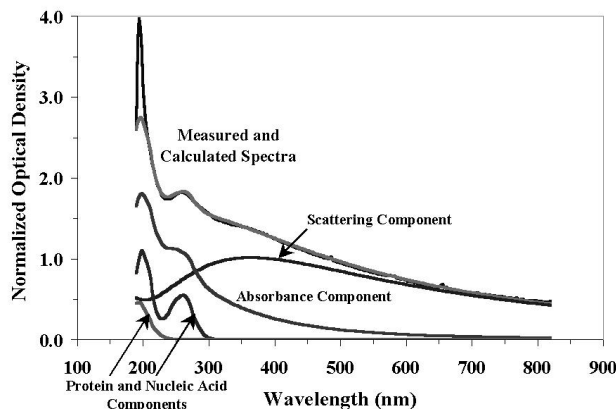


Figure 6: Deconvolution of the *Cryptosporidium* transmission spectrum

the output from the interpretation is shown in Figure 7. Note how detailed the information is. The fact that such a large amount of information is contained in such a simple measurement is one of the advantages associated with our characterization approach. In the case of *Cryptosporidium*, the internal scattering elements characterized by the model are suspected to be regions of concentrated nuclear material. Note that the size estimate (4.07  $\mu\text{m}$ ) and nucleic acid content estimate (0.94 pg/cell) obtained with the model agree with literature values reported for *Cryptosporidium*.

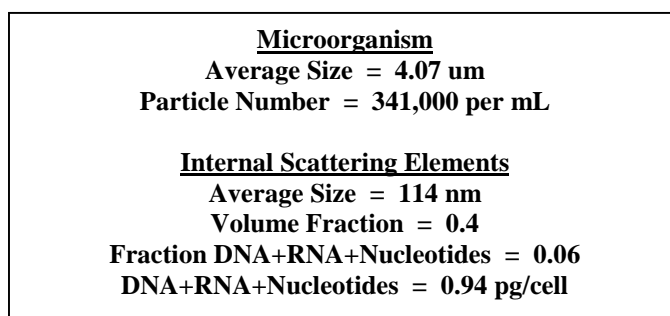


Figure 7: Detailed information contained in the transmission spectra for *Cryptosporidium*

## 5. CONCLUSIONS AND WORK IN PROGRESS

As shown in this paper, even at the qualitative level, multiwavelength transmission spectra can be used to distinguish between different cell types. When these spectroscopic differences are translated into quantitative estimates of particle properties, important information for the detection, identification and classification of the cells is obtained. The ability to discriminate between cell types was demonstrated with the light scattering and absorption interpretation model and optical properties developed in our laboratory. Estimates of average particle size, particle number and chemical composition were obtained using our approach. In the case of *Cryptosporidium*, the absorbance components of the spectrum have been deconvoluted into more detailed compositional information on protein and nucleic acid content. With this level of detail in the analysis, the multiwavelength UV/vis approach has the potential to provide a sensitive biosensor for the detection, identification and enumeration of pathogens.

Work in progress includes developing the necessary interpretation models for samples contained in dense media such as meat. In addition, work investigating the sensitivity of the approach is also underway. An effective biosensor must be able to detect low numbers of pathogens. Other areas of interest are in the spectroscopic characterization of viable versus

nonviable cells and in the detection of specific pathogens in a mixture of microorganisms. These issues and others must be investigated if our multiwavelength spectroscopic approach is going to provide an effective biosensor that is precise, reliable, rapid and sensitive. The results presented here support the potential of our approach to provide a novel biosensor for pathogen detection and identification.

## ACKNOWLEDGEMENTS

The authors would like to acknowledge the support of Los Alamos National Laboratory, American Water Works Research Foundation and the Engineering Research Center (ERC) for Particle Science and Technology at the University of Florida.

## REFERENCES

1. L. H. Garcia-Rubio, C. A. Lopez-Menacho and S. Grossman, "Characterization of proteins during aggregation II: Use of model molecules for spectroscopy analysis," *Chem. Eng. Comm.* **122**, pp. 85-101, 1993.
2. M. R. Callahan, R. Robertson, J. B. Rose and L.H. García-Rubio, "Characterization of *Cryptosporidium* by ultraviolet visible light spectroscopy," Manuscript in preparation.
3. C. Bacon, J.B. Rose, K. Patten and L. H. Garcia-Rubio, "Quantitative classification of *Cryptosporidium* oocysts and *Giardia* cysts in water using uv/vis spectroscopy," *Proc. SPIE* **2388**, pp. 471-480, 1995.
4. Y. Mattley, G. Leparc, R. Potter and L. Garcia-Rubio, "Light scattering and absorption model for the quantitative interpretation of human blood-platelet spectral data," *Photochem. Photobiol.* **71(5)**, pp. 610-619, 2000.
5. H.C. van de Hulst, *Light Scattering by Small Particles*, Wiley, New York, 1957.
6. D. H. Melik and H. S. Fogler "Determination of particle size distribution in colloid systems," *J. Colloid Interf. Sci.* **92**, pp. 161-180, 1983.
7. M. Kerker *The Scattering of Light and Other Electromagnetic Radiation*, Pergamon Press, New York, 1969.
8. M. L. Wallach and W. Heller "Theoretical investigations on the light scattering of colloidal spheres XII: The determination of size distribution curves from turbidity spectra," *J. Chem. Phys.* **24(5)**, pp. 1796-1802, 1961.
9. R. L. J. Zollars "Turbidimetric method for on-line determination of latex particle number and particle size distribution," *J. Coll. Interface Sci.* **74**, pp. 163-172, 1980.
10. S. Towmey *Introduction to the Mathematics of Inversion in Remote Sensing and Indirect Measurements*, Elsevier, New York, 1979
11. A. Tarantola *Inverse Problem Theory*, Elsevier, Amsterdam, 1987.
12. G. E. Elicabe and L. H. Garcia-Rubio, "Latex particle size distribution from turbidimetry using inversion techniques," *J. Colloid Interf. Sci.* **129**, pp. 192-200, 1988.
13. G. Elicabe and L. H. García-Rubio "Latex particle size distribution from turbidimetric measurements combining regularization and generalized cross-validation techniques," *Adv. Chem. Ser.* **227**, pp. 83-104, 1990.
14. A. Brandolin, L. H. Garcia-Rubio, T. Provder, M. E. Kohler and C. Kuo, "Latex particle size distribution from turbidimetry using inversion techniques, experimental validation", In *Particle Size Distribution II: Assessment and Characterization* (Edited by T. Provder) *ACS Symposium Series* **472**, pp. 20-33, 1991.
15. Y. Koumarioti, L. M. Davis, S. Chang and L. H. García-Rubio "Spectroscopy analysis of particle suspensions" In *Proceedings of the Engineering Foundation Conference on Development of Non-Renewable Resources: Challenges and Solutions* (Edited by H. El Shall, A. Ismail, B. Moudgil), pp. 83-92. United Engineering Foundation, Inc., New York, 1999.
16. G. H. Golub, M. Heath and G. Wahba, "Generalized cross validation as a method for choosing a good ridge parameter," *Technometrics* **21**, pp. 215, 1979.
17. L. H. García-Rubio, "The effect of the molecular size on the absorption spectra of macromolecules," *Macromolecules* **20**, pp. 3070-3075, 1987.
18. I. Thormählen, J. Straub and U. J. Grigull "Refractive index of water and its dependence on wavelength, temperature, and density," *J. Phys. Chem. Ref. Data* **14**, 933-945, 1985.
19. G. R. Lee, T. C. Bithell, J. Foerster, J. W. Athens and J. N. Lukens *Wintrobe's Clinical Hematology 9th edition*, Volume 1 pp. 515. Lea and Febiger, Philadelphia, 1992.
20. R. L. Adams, J. T. Knowler and D. P. Leader *The Biochemistry of Nucleic Acids 10th edition*, McGraw Hill, New York, 1989.
21. D. Freifelder *Physical Biochemistry 2nd edition* Chapter 14 pp. 504. W.H. Freeman and Company, 1982.
22. J. Sambrook, E. F. Fritsch and T. Maniatis "Spectrophotometric determination of the amount of DNA and RNA" In *Molecular Cloning 2nd edition*. Appendix E.5. Cold Springs Harbor Laboratory Press, 1989.